arXiv:0806.2219v1 [cond-mat.str-el] 13 Jun 2008

Quantum Monte Carlo Study of the Quasi-One-Dimensional Superconductivity

Tohru AONUMA, Yuki FUSEYA and Masao OGATA

Department of Physics, University of Tokyo, Hongo, Bunkyo-ku, Tokyo 113-0033

We report on the result of quantum Monte Carlo simulation of quasi-one-dimensional electron systems at 1/4-filling, considering organic superconductors such as TMTSF- and TMTTF-salts. We focus on the effect of dimensionality (interchain coupling) on superconducting fluctuation. First we consider Hubbard model which includes only on-site repulsion U. We find that the increase of interchain coupling enhances superconducting susceptibility, although it deforms the nested Fermi surface and suppresses the spin susceptibility. Next we consider an extended Hubbard model which includes nearest-neighbor repulsion V. In this case we consider the competition between different symmetries of electron pairing, $d_{x^2-y^2}$- and d_{xy}-wave symmetry, and find that the particle-particle interaction vertex for $d_{x^2-y^2}$-wave pairing is no longer attractive even in the region where nesting condition still holds. On the other hand, the interaction vertex for d_{xy}-wave pairing persists to be attractive. The obtained results for the Hubbard model show qualitative agreement with recent renormalization group study, and have the possibility of accounting for the recent experimental result of $(TMTTF)_2SbF_6$, which exhibits a wider superconducting phase than the previous studies.

KEYWORDS: superconductivity, quasi-one-dimension, extended Hubbard model, quantum Monte Carlo, organic conductors, TMTSF, TMTTF

1. Introduction

Quasi-one-dimensional (Q1D) electron systems, such as organic conductors TMTSF- and TMTTF-salts (TM_2X), have been extensively studied both theoretically and experimentally after the discovery of superconductivity in $(TMTSF)_2PF_6$.[1] Various experiments have been carried out and the results are summarized as the so-called Jérome's phase diagram.[2] In this generic diagram, the ground state changes as spin-Peierls, spin-density-wave (SDW) and superconductivity (SC) by applying pressure. The SC phase is located next to the SDW phase; it suggests that the source of the attractive interaction between electrons is due to antiferromagnetic spin fluctuation. The fact that the SC transition temperature, T_c, decreases as applying pressure (going away from SDW phase) supports this prediction. Many theoretical studies have been performed from this point of view [3–7] and the obtained results give qualitative agreement with the experiments.

A recent experimental result exhibits, however, a wider SC phase under high-pressure.[8] This suggests that the effect of pressure (or increase of interchain hopping) on SC phase is positive. From the theoretical point of view, the possibility of higher T_c due to the increase of interchain hopping has been proposed from the early days on the basis of one-dimensional (1D) renormalization group theory.[9] Recently, modification of this approach makes it possible to treat strong quantum fluctuations in Q1D system,[10] and concludes that the $d_{x^2-y^2}$-wave pair-field susceptibility shows clear enhancement against interchain hopping.[11,12] It indicates that the decline of T_c along pressure may not be the case.

However, the previous studies are mainly based on the perturbative methods, especially the ones which focus on the spin fluctuation. Although it has been verified that the results of these approaches qualitatively agree with that of numerical methods in two-dimensional systems,[13] it has not been confirmed yet whether these approximations are good in 1D or Q1D systems. The main obstacle is the strong quantum fluctuations in these systems, i.e., spin fluctuation and the other types of fluctuations are competitive and they interfere with each other. One of the methods which can treat these fluctuations correctly is the Q1D renormalization group theory mentioned above. However, it has its origins in the 1D renormalization and is applicable only to weakly-coupled chains. Thus, in this paper, we adopt the quantum Monte Carlo (QMC) method in order to treat not only the spin fluctuation but also all types of fluctuations at the same weight, which is rather difficult in perturbative approaches such as RPA or FLEX approximation. In addition, it can treat any strength of interchain coupling without approximation in contrast to the Q1D renormalization group theory. We investigate the effect of interchain hopping, or dimensionality, on the SC fluctuation in the Hubbard model by using the auxiliary field QMC,[14,15] having in mind the SC phase of TM_2X salts under pressure.

Furthermore, we study the effect of long range Coulomb interaction V, which has been recognized to be very important in organic conductors, especially the TMTTF-salts, in the context of the charge ordering (CO).[16,17] So far, the effect of V on the SC has been investigated for the SC phase next to the CO phase, such as α-ET_2I_3,[18–20] or β-$(DMeET)_2PF_6$.[21] As for TM_2X salts, on the other hand, it has not been studied since the SC phase is separated from the CO phase. However, the high-energy peak ($\sim$ 30meV) of the optical conductivity has been observed even in the metallic $TMTSF_2X$ salts,[22] indicating a precursor of CO. The effect of V, therefore, is not negligible even in the metallic Q1D compounds; it can give an sizable impact on the mechanism

of SC. In order to clarify this effect, we also investigate the behavior of SC susceptibility for the Q1D extended Hubbard model.

This paper is organized as follows. In §2, we introduce the model and method used in this paper. In §3, the results of the Hubbard model are presented, which correspond to the situation similar to the previous studies. They show qualitative agreement with the renormalization group study.[12] In §4, the result of the extended Hubbard model is presented. The effect of V mainly appears as the change of SC symmetry from $d_{x^2-y^2}$ to d_{xy}. The comparison with the experimental results is given in §5.

2. Model and Method

We consider the two-dimensional Hubbard and extended Hubbard model on an anisotropic square lattice, whose Hamiltonian is given by

$$H = \sum_{\langle ij\rangle\sigma}\left(-t_{ij}c^{\dagger}_{i\sigma}c_{j\sigma} + \text{h.c.}\right) + U\sum_{i} n_{i\uparrow}n_{i\downarrow} + V\sum_{\langle ij\rangle\sigma\sigma'} n_{i\sigma}n_{j\sigma'} - \mu\sum_{i\sigma} n_{i\sigma}, \tag{1}$$

where $c^{\dagger}_{i\sigma}$ ($c_{i\sigma}$) is the creation (annihilation) operator of an electron with spin σ ($\sigma =\uparrow,\downarrow$) on site i and $n_{i\sigma} = c^{\dagger}_{i\sigma}c_{i\sigma}$. Here t_{ij} has two different values, t_x (intrachain hopping) and t_y (interchain hopping). The nearest-neighbor Coulomb interaction V is introduced as depicted in Fig. 1. We set the intrachain hopping $t_x = 1$,

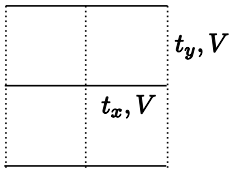


Fig. 1. Transfer integrals t_x, t_y and nearest-neighbor repulsion V.

interaction strength $U = 4$ and $k_{\rm B} = \hbar = 1$ throughout this paper. The number of electrons are set to be $\langle n\rangle = 1/4$ by tuning the chemical potential μ.

In order to investigate the properties of this model, we employ the auxiliary field quantum Monte Carlo method.[14,15] The shape of the cluster is set to be 16×8 for $V = 0$ or 16×4 for $V \neq 0$. It means that there are 16 sites along chains (x-direction) and 8 (or 4) chains are coupled with each other in the y-direction. In the presence of V, we restrict the system size to 16×4 and the temperature range to $\beta(= 1/T) \leq 4$, because of heavy computational cost of Monte Carlo sampling.[25] The imaginary-time step is set to be $\Delta\tau = 1/8$, and 64000 measurements separated by two sweeps are performed after 1000 warm-up.

We calculate spin, charge and pair-field susceptibilities

$$\chi_{\rm s}(\boldsymbol{q}) = \frac{1}{N}\int_0^{\beta} \mathrm{d}\tau \sum_{ij} \mathrm{e}^{\mathrm{i}\boldsymbol{q}\cdot(\boldsymbol{r}_i-\boldsymbol{r}_j)}\langle m^z_i(\tau)m^z_j(0)\rangle,$$

$$\chi_{\rm c}(\boldsymbol{q}) = \frac{1}{N}\int_0^{\beta} \mathrm{d}\tau \sum_{ij} \mathrm{e}^{\mathrm{i}\boldsymbol{q}\cdot(\boldsymbol{r}_i-\boldsymbol{r}_j)}\langle \tilde{n}_i(\tau)\tilde{n}_j(0)\rangle,$$

$$\chi_{d\rm SC} = \frac{1}{4N}\int_0^{\beta} \mathrm{d}\tau \sum_{ij}\langle \Delta_i(\tau)\Delta^{\dagger}_j(0)\rangle \tag{2}$$

with

$$m^z_i(\tau) = c^{\dagger}_{i\uparrow}(\tau)c_{i\uparrow}(\tau) - c^{\dagger}_{i\downarrow}(\tau)c_{i\downarrow}(\tau),$$

$$\tilde{n}_i(\tau) = c^{\dagger}_{i\uparrow}(\tau)c_{i\uparrow}(\tau) + c^{\dagger}_{i\downarrow}(\tau)c_{i\downarrow}(\tau) - \langle n\rangle,$$

$$\Delta_i(\tau) = \sum_{\delta} f_d(\delta)c_{i\uparrow}(\tau)c_{i+\delta\downarrow}(\tau).$$

Here $f_d(\delta)$ is the factor $+1$ or -1 corresponding to the pairing symmetries as shown in Fig. 2.

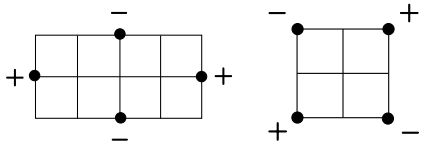


Fig. 2. The internal pair coordinate δ and the factor $f_d(\delta)$ used in defining Δ_i for $d_{x^2-y^2}$-wave pairing (left panel) and d_{xy}-wave pairing (right panel).

In addition to eq. (2), we also calculate the uncorrelated pair-field susceptibility[26,27]

$$\bar{\chi}_{d\rm SC} = \frac{1}{4N}\int_0^{\beta} \mathrm{d}\tau \sum_{i\delta j\delta'} f_d(\delta)f_d(\delta') \times \underbrace{\langle c_{i\uparrow}(\tau)c^{\dagger}_{j\uparrow}(0)\rangle}_{-G_{i,j,\uparrow}(\tau)} \underbrace{\langle c_{i+\delta\downarrow}(\tau)c^{\dagger}_{j+\delta'\downarrow}(0)\rangle}_{-G_{i+\delta,j+\delta',\downarrow}(\tau)}. \tag{3}$$

The difference between eqs. (2) and (3) is whether the particle-particle vertex Γ is included or not (see Fig. 3). If

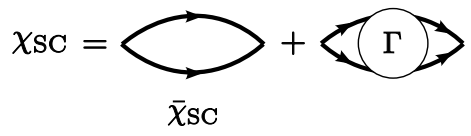


Fig. 3. Full susceptibility $\chi_{\rm SC}$ and uncorrelated susceptibility $\bar{\chi}_{\rm SC}$. Thick lines denote the dressed Green's functions. Γ is the particle-particle interaction vertex.

$\chi_{\rm SC}$ is larger than $\bar{\chi}_{\rm SC}$, it means that Γ is attractive.[26–28]

We also calculate the density of states $N(\omega)$, which is defined as

$$\sum_i G_{ii}(\tau) = -\int_{-\infty}^{\infty} \mathrm{d}\omega \frac{\mathrm{e}^{-\omega\tau}}{1+\mathrm{e}^{-\beta\omega}} N(\omega), \tag{4}$$

where $G_{ij}(\tau)$ is the imaginary-time Green's function

$$G_{ij}(\tau) = -\sum_{\sigma}\langle c_{i\sigma}(\tau)c^{\dagger}_{j\sigma}(0)\rangle.$$

This expression will be readily understood from the definition of $N(\omega)$

$$N(\omega) = \frac{1}{N}\sum_{\boldsymbol{k}} A(\boldsymbol{k},\omega)$$

with $A(\boldsymbol{k},\omega)$ being the one-particle excitation spectrum

$$G(\boldsymbol{k},\tau) = -\int_{-\infty}^{\infty} \mathrm{d}\omega \frac{\mathrm{e}^{-\omega\tau}}{1+\mathrm{e}^{-\beta\omega}} A(\boldsymbol{k},\omega).$$

The inverse transformation from $G_{ii}(\tau)$ to $N(\omega)$ in eq. (4) is carried out by the maximum entropy method combined with QMC.[29]

3. Results of the Hubbard model

First we show the results of the Hubbard model, whose Hamiltonian is given by eq. (1) with $V = 0$. Figure 4 is the spin susceptibility $\chi_{\rm s}(\boldsymbol{Q})$ and SC susceptibility $\chi_{d\rm SC}$ against temperature T for different values of t_y. As for

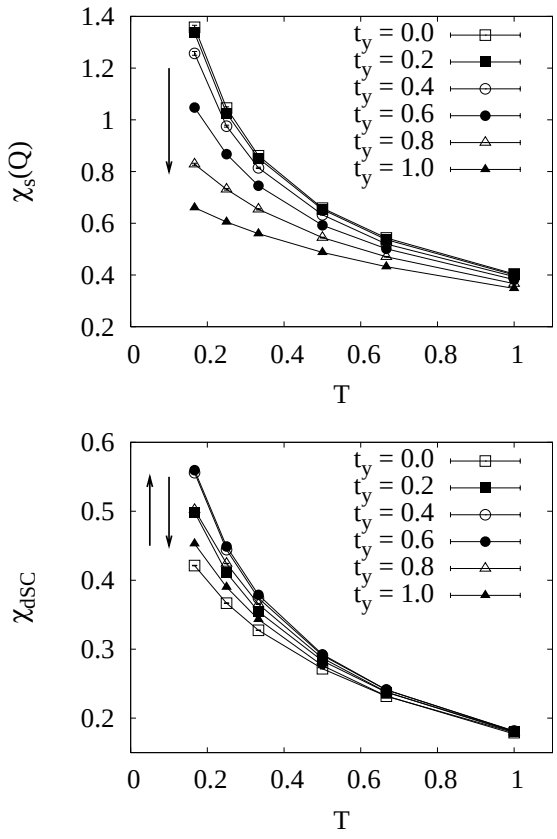


Fig. 4. Temperature dependences of spin susceptibility $\chi_{\rm s}(\boldsymbol{Q})$ (upper panel) and $d_{x^2-y^2}$-wave pair-field susceptibility $\chi_{d\rm SC}$ (lower panel) for $U = 4$ and different values of t_y. The change of these susceptibilities when t_y is increased are indicated by arrows. Where not shown, error bars are smaller than the symbols.

$\chi_{\rm s}(\boldsymbol{Q})$, it is strongly enhanced at low temperature near

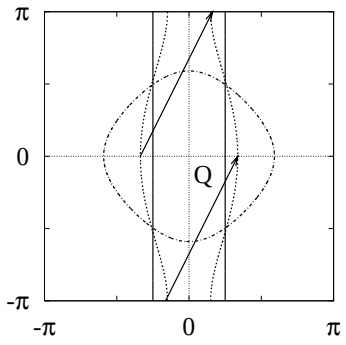


Fig. 5. Fermi surfaces with $t_y = 0.0$ (solid), 0.2 (dotted) and 1.0 (dash-dotted) at 1/4-filling. The good nesting condition holds at about $0.0 \le t_y \le 0.3$. $\boldsymbol{Q} = (\pi/2, \pi)$ is a nesting vector.

1D, but the enhancement becomes moderate as t_y increases. This is due to the breaking of the nesting condition, as depicted in Fig. 5. On the other hand, $\chi_{d\rm SC}$ shows different behaviors. $\chi_{d\rm SC}$ is *enhanced* by t_y in small t_y region, while $\chi_{\rm s}(\boldsymbol{Q})$ decreases. $\chi_{d\rm SC}$ becomes largest at the intermediate values of t_y, such as $t_y = 0.4$ or 0.6.

The t_y-dependences of $\chi_s(\boldsymbol{Q})$ and $\chi_{d\rm SC}$ are summarized in Fig. 6 when the temperature is fixed at $T = 0.167$. The non-monotonic behavior of $\chi_{d\rm SC}$ can be in-

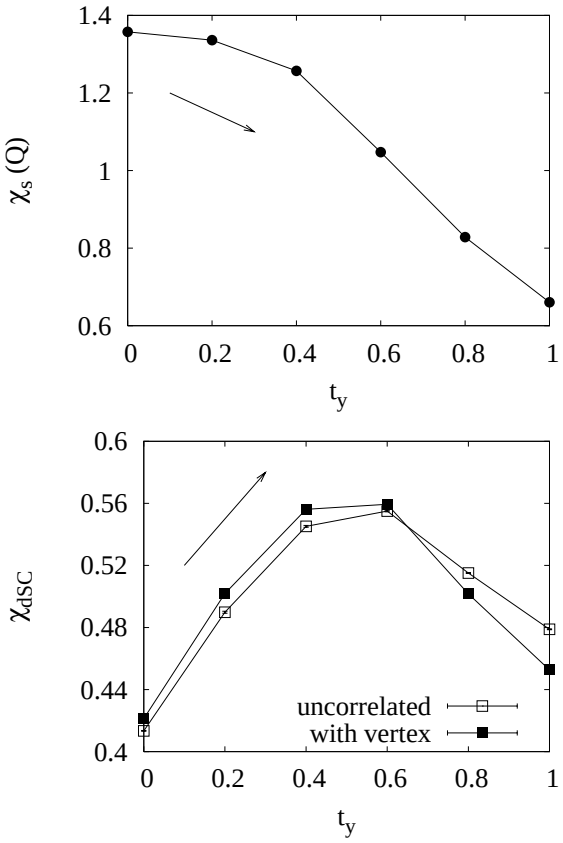


Fig. 6. t_y-dependences of spin susceptibility $\chi_{\rm s}(\boldsymbol{Q})$ (upper panel) and $d_{x^2-y^2}$-wave pair-field susceptibility $\chi_{d\rm SC}$ (lower panel, solid squares) at $T = 0.167$ for $U = 4$. The open squares denote the uncorrelated pair-field susceptibility $\bar{\chi}_{d\rm SC}$.

terpreted as follows: the enhancement comes from the pair-hopping of electrons, and the suppression is due to the suppression of spin fluctuation because of the deformation of the nested Fermi surface. In fact, the peak position of $\chi_{\rm s}(\boldsymbol{q})$ locates at around $\boldsymbol{q} = \boldsymbol{Q}$ for $0.0 \leq t_y \leq 0.6$, while it does not at $t_y = 0.8$ and 1.0 (not shown).

In Fig. 6, the uncorrelated susceptibility, $\bar{\chi}_{d\rm SC}$, is also shown in comparison with the full susceptibility, $\chi_{d\rm SC}$. We find that the vertex part is attractive for $0.0 \leq t_y \leq 0.6$, while it is repulsive for $t_y = 0.8$ and 1.0. This is consistent with the above picture that $\chi_{d\rm SC}$ is most enhanced at the region where the nesting property and the interchain pair-hopping of electrons are well balanced.

In order to confirm the effect of nesting property, it is useful to introduce the frustrated hopping, t', as shown in Fig. 7. This kind of hopping is another key to control the

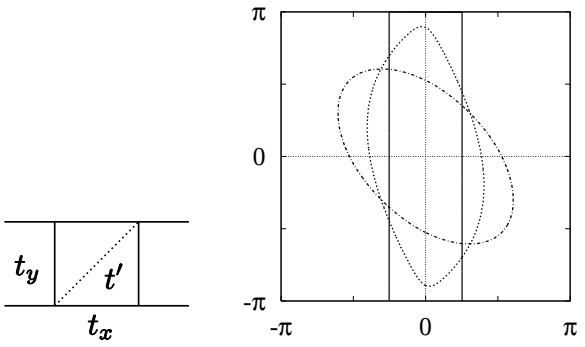


Fig. 7. Left panel: the interchain hopping t', which induces geometrical frustration. Right panel: Fermi surfaces with frustration t' when $t_y = 0.0$ (solid), $t_y = 0.2$ (dotted) and 1.0 (dash-dotted) at 1/4-filling. The value of t' is chosen as $t' = t_y/2$. It should be noted that the nesting vector $\boldsymbol{Q}$ no longer exists.

strength of spin fluctuation and interchain coupling. In fact, this type of transfer integral has been confirmed to exist in many TM_2X-salts.[30] It deforms the Fermi surface and worsen the nesting condition (compare Fig. 5 and 7).

Figure 8 shows the t_y-dependence of spin and SC susceptibilities at $T = 0.167$ for different strengths of t'. Here we choose the values of t' as $t' = 0$, $t_y/2$ and t_y. It is seen that $\chi_{d\rm SC}$ is slightly enhanced at small t_y region and suppressed at large t_y region, while $\chi_{\rm s}(\boldsymbol{Q})$ is monotonically suppressed by t'. The enhancement of $\chi_{d\rm SC}$ will be again due to the increase of interchain coupling. Indeed, the interchain hopping t' couples the chains more tightly, while it worsen the nesting condition. It will increase the pair-hopping of electrons and, as a result, $\chi_{d\rm SC}$ is slightly enhanced by t'. In addition, the region where the interaction vertex is attractive ($\chi_{d\rm SC} - \bar{\chi}_{d\rm SC} > 0$) shifts to the smaller t_y region (not shown), which simply supports this picture.

However, one might point out that the maximum of $\chi_{d\rm SC}$ is due to the van Hove singularity which exists at $t_y \sim 0.35$ in 1/4-filled non-interacting system, i.e., the effect of electron-electron interaction does not matter. In order to clarify this point, we calculate the density

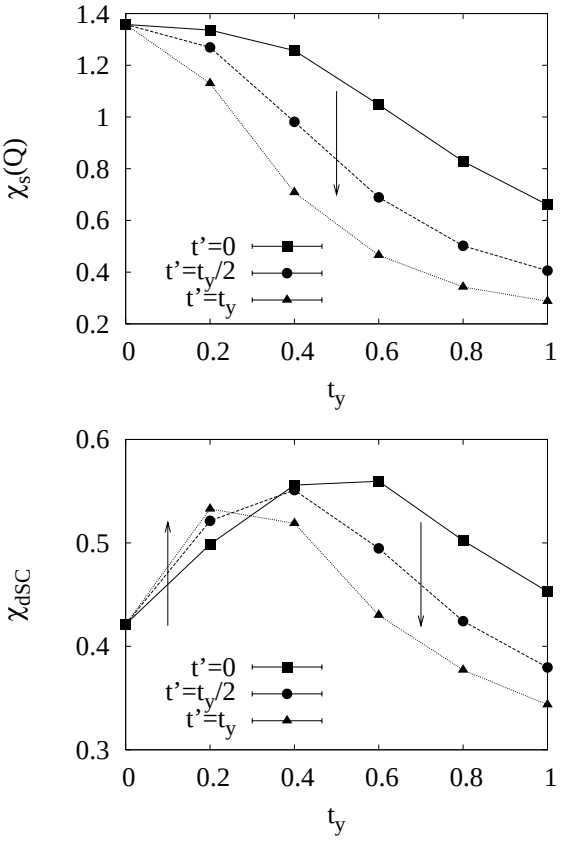


Fig. 8. t_y-dependences of spin susceptibility $\chi_{\rm s}(\boldsymbol{Q})$ (upper panel) and $d_{x^2-y^2}$-wave pair-field susceptibility $\chi_{d\rm SC}$ (lower panel) at $T = 0.167$ for $U = 4$. Squares, circles and triangles correspond to the case $t' = 0$, $t_y/2$ and t_y. The change of these susceptibilities when t' is strengthened are indicated by arrows.

of states (DOS) $N(\omega)$ for interacting system. Figure 9 shows $N(\omega)$ at $T = 0.167$ for different values of t_y (here we consider the case $t' = 0$). Although the suppression of $N(\omega = \mu)$ at large t_y region is recognized, the enhancement at small t_y region seems not to exist. This behavior does not follow the curve of $\chi_{d\rm SC}$ against t_y. Thus we conclude that the effect of van Hove singularity is irrelevant to understand the non-monotonic behavior of $\chi_{d\rm SC}$, as long as the temperature range we calculated.

4. Results of the extended Hubbard model

In the previous section, we investigate the case with $V = 0$, where $\chi_{d\rm SC}$ is affected by the pair-hopping of electrons, in addition to the strength of spin fluctuation. On the other hand, the pairing mechanism itself is well understood by the spin-fluctuation theory. In this section, we consider whether this pairing mechanism is valid or not under the presence of charge fluctuation induced by the nearest-neighbor repulsion V.

We consider the extended Hubbard model, whose Hamiltonian is given by eq. (1). We impose the limitation on not only the system size and temperature but also V as $V \leq 0.5$ in order to avoid round-off errors and severe sign problem. (We adopt the parameters which assure that the average sign $\langle S \rangle$ becomes greater than 0.1.)

First we show the spin and charge susceptibilities with and without V. The upper two panels of Fig. 10 rep-

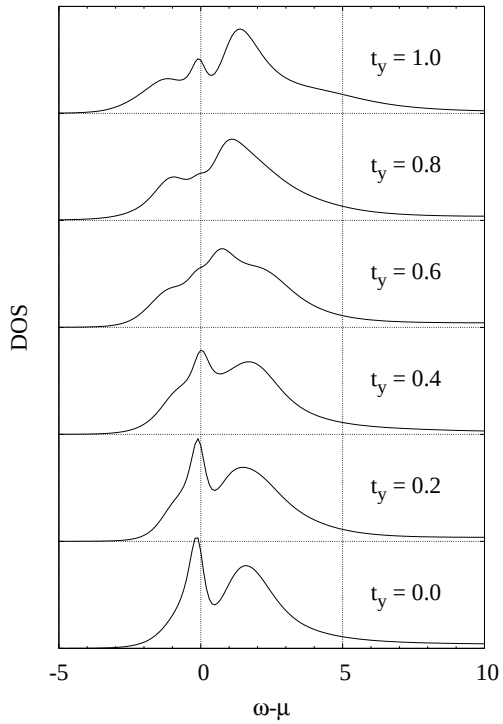


Fig. 9. Density of States for $U = 4$ and different values of t_y at $T = 0.167$. The frustration t' is not included.

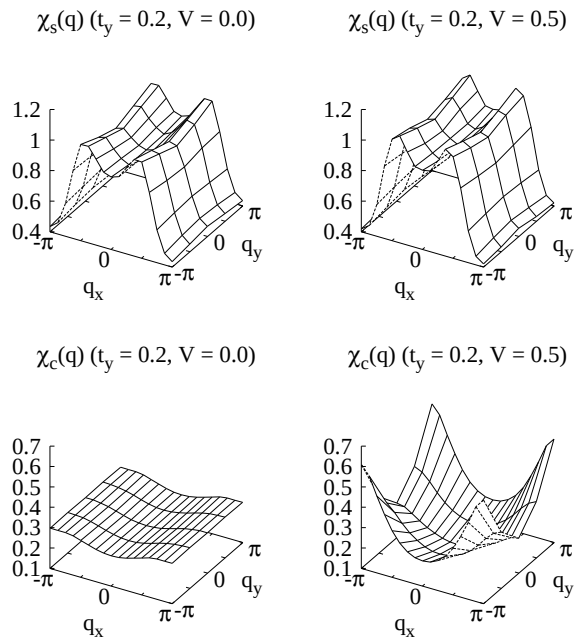


Fig. 10. Spin susceptibility $\chi_{\rm s}(\boldsymbol{q})$ (upper panels) and charge susceptibility $\chi_{\rm c}(\boldsymbol{q})$ (lower panels) when $T = 0.25$ and $t_y = 0.2$ in the 1st Brillouin zone. The interaction strengths are $U = 4$, $V = 0$ (left panels) and $U = 4$, $V = 0.5$ (right panels). The structure of $\chi_{\rm s}(\boldsymbol{q})$ reflects the shape of the nested Fermi surface with a nesting vector $\boldsymbol{Q} = (\pi/2, \pi)$ and seems not to be affected by V. On the other hand, the structure of $\chi_{\rm c}(\boldsymbol{q})$ is largely affected by V and its peak position reflects the geometrical structure of V (or its Fourier transform $V(\boldsymbol{q}) \propto \cos(q_x) + \cos(q_y)$). Note that each point includes errors with a few percent.

resent the spin susceptibility, $\chi_{\rm s}(\boldsymbol{q})$, for $V = 0$ and 0.5 when $T = 0.25$ and $t_y = 0.2$, where the temperature is relatively low and the nesting condition still holds. It is seen that the structure of $\chi_{\rm s}(\boldsymbol{q})$ is hardly affected by V. It comes from the fact that $\chi_{\rm s}(\boldsymbol{q})$ is mainly affected by the shape of the Fermi surface, which is considered not to be drastically deformed by V. The lower two panels of Fig. 10 show the charge susceptibility, $\chi_{\rm c}(\boldsymbol{q})$. A sharp peak at $\boldsymbol{q} = (\pi, \pi)$ is formed when V is finite, which is considered to be the reflection of the lattice structure. (Note that we consider the 1/4-filled system, which favors $\boldsymbol{q} = (\pi, \pi)$ charge disproportionation under finite V.) This result suggests that the charge fluctuation induced by V is more affected by the geometrical configuration of V rather than the shape of the Fermi surface.[31] It is a clear contrast between $\chi_{\rm s}$ and $\chi_{\rm c}$: the nesting property (momentum space) and the lattice structure (real space).

It is an interesting subject to investigate how V affects SC susceptibility. To understand the effect of charge fluctuation, we consider not only the $d_{x^2-y^2}$-wave pairing but also d_{xy}-wave pairing, whose gap function Δ_i is defined in Fig. 2. Figure 11 shows the temperature dependence of the SC susceptibilities for these two pairings. They are qualitatively similar, but it seems that d_{xy}-wave pairing is slightly larger than the $d_{x^2-y^2}$-wave pairing. This advantage of d_{xy}-wave pairing over $d_{x^2-y^2}$-wave pairing will be recognized more clearly in Fig. 12, where the t_y-dependences of these susceptibilities at $T = 0.25$ are shown. (The results without V are also displayed for comparison.) The $d_{x^2-y^2}$-wave pairing is drastically suppressed by V, although the suppression of d_{xy}-wave pairing is not so large. Furthermore, it should be noted that, for $V = 0.5$, the interaction vertex for $d_{x^2-y^2}$-wave pairing is repulsive for *any* value t_y, even for $t_y = 0.0$ or 0.2 where strong spin fluctuation still exists. This suggests that the spin and charge fluctuations cancel each other and the vertex part for $d_{x^2-y^2}$-wave pairing is no longer attractive. On the other hand, the interaction vertex for the d_{xy}-wave pairing is still attractive; it is even enhanced at the region of large t_y.

Finally, we estimate the effects of V on the dynamical property of this model. Figure 13 shows the DOS, $N(\omega)$, for different values of t_y at $T = 0.25$ and $V = 0.5$. Note that $N(\omega = \mu)$ on the Fermi surface is finite for any value of t_y, i.e., the system is metallic and the CO does not occur. It is surprising that such a small V largely affects the SC interaction vertex.

In this section we have investigated the effect of charge fluctuation induced by the nearest-neighbor repulsion V on the SC symmetry. Our results indicate that the symmetry of electron pair changes from $d_{x^2-y^2}$ to d_{xy}, even if there still exists strong spin fluctuation and V is as weak as not accompanying CO. It suggests that the effect of V on SC is not negligible, even in the metallic system with strong spin fluctuation. We should incorporate not only the shape of the Fermi surface but also the effect of $V(\boldsymbol{q})$ into discussion.

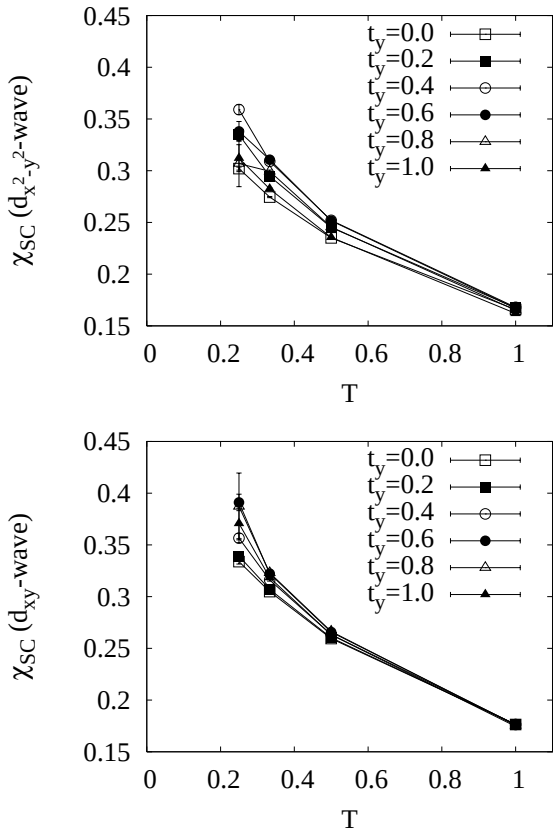


Fig. 11. Temperature dependences of SC susceptibility for $d_{x^2-y^2}$-wave (upper panel) and d_{xy}-wave (lower panel) pairings for $\langle n \rangle = 0.5$, $U = 4$ and $V = 0.5$.

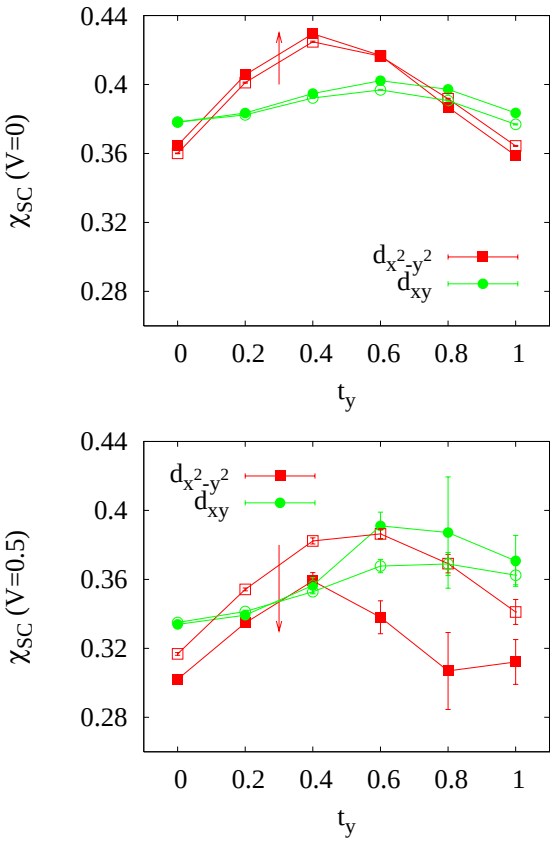


Fig. 12. (Color online) t_y-dependence of SC susceptibility at $T = 0.25$ for $U = 4$, $V = 0.0$ (upper panel) and $U = 4$, $V = 0.5$ (lower panel). The solid and open symbols denote the full and uncorrelated susceptibility. The contribution of particle-particle interaction vertex for $d_{x^2-y^2}$-wave pairing is indicated by arrows: attractive (upper panel) and repulsive (lower panel).

5. Conclusions

In this paper we have investigated the superconductivity in Q1D system from the non-perturbative point of view, focusing on the effect of dimensionality on SC fluctuation. First we introduced the result of the Hubbard model, which includes only the on-site repulsion U. In this case, it is found that the $d_{x^2-y^2}$-wave pair-field susceptibility, $\chi_{d\mathrm{SC}}$, is increased by t_y in the small t_y region, while the spin fluctuation $\chi_{\mathrm{s}}(\boldsymbol{Q})$ is monotonically suppressed by t_y. This behavior comes from the fact that the increase of t_y has two different effects; the deformation of the Fermi surface and the enhancement of pair-hopping of electrons. The $d_{x^2-y^2}$-wave SC is most enhanced at the region where these two factors are well balanced, as shown in the left panel of Fig. 14 schematically. This behavior suggests that the monotonic decline of T_{c} may not be the case. On the other hand, the pairing mechanism itself is the well-known spin fluctuation assumed by many previous studies. It is confirmed by the fact that the shape of the Fermi surface determines whether the particle-particle interaction vertex Γ for $d_{x^2-y^2}$-wave pairing is attractive or not.

Next we considered the effect of nearest-neighbor repulsion V, focusing on the effect of charge fluctuation induced by V on the symmetry of electron pair. The expected behavior for d_{xy}-wave pairing is shown in the right panel of Fig. 14. We speculate that the charge fluctuation induced by V is not affected by the nesting property of

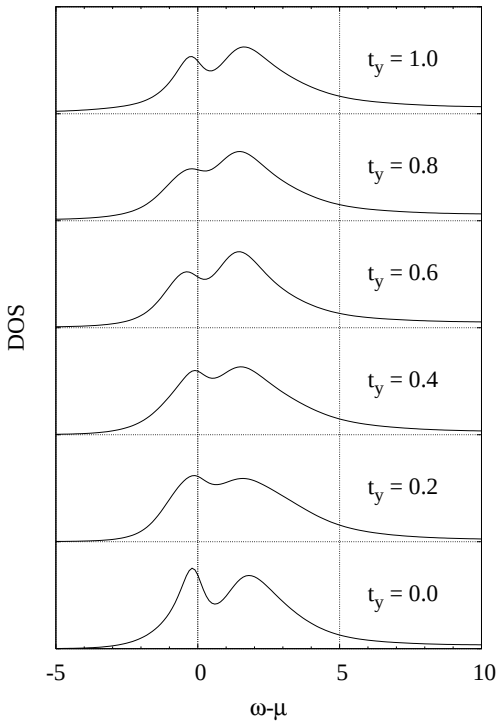


Fig. 13. Density of states at $T = 0.25$ for $U = 4$ and $V = 0.5$.

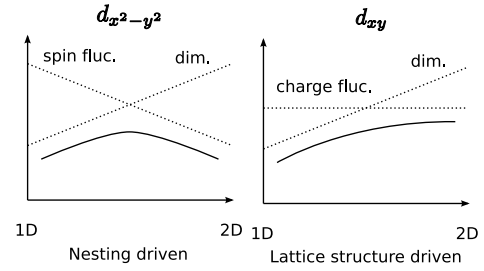


Fig. 14. Schematic representation of the effect of dimensionality on SC fluctuation in Q1D 1/4-filled system.

the Fermi surface but the geometrical lattice structure. In this case, the increase of t_y simply makes a positive contribution to SC because of the enhancement of the electron pair-hopping. Our results support this picture, and in addition, indicate that Γ for $d_{x^2-y^2}$-wave pairing is repulsive when V is finite, even at the region where strong spin fluctuation still exists and V is as small as not accompanying CO. On the other hand, d_{xy}-wave pairing is not so largely affected by V and Γ for d_{xy}-wave pairing remains attractive. This indicates that the nesting property is not necessarily the crucial factor for determining the symmetry of electron pair, even if the system has a good nesting property. It may sound peculiar, especially from the perturbative point of view which focuses on the pairing mechanism mediated by the fluctuation of the ordered phase next to the SC. However, the possibility of strong cancellation between spin and charge fluctuations in Γ would not be so unrealistic. It suggests that we should incorporate the effect of long range Coulomb interaction V into the discussion of SC in order to determine the symmetry of electron pair.

Let us compare our results with experiment. We showed that the $\chi_{d\mathrm{SC}}$ is enhanced by increasing t_y, whichever the symmetry of electron pair is $d_{x^2-y^2}$ or d_{xy}. It suggests that the SC phase in TM_2X salts have the possibility of becoming wider, such as what is confirmed in $(TMTTF)_2SbF_6$.[8] Furthermore, we also found that the d_{xy}-wave pairing becomes more realistic than $d_{x^2-y^2}$-wave pairing under the presence of nearest-neighbor repulsion V. It indicates that the $d_{x^2-y^2}$-wave pairing which is assumed in the previous studies of TM_2X-salts may need to be revised. In fact, not only the TMTTF-salts, the TMTSF-salts showing the metallic behavior at ambient pressure have the precursor of CO as the higher-energy peak of the optical conductivity.[22] This means that the long-range Coulomb interaction is not negligible in not only TMTTF-salts but also TMTSF-salts.

Finally, let us comment on the temperature range of the present calculation. We cannot study very low temperature region due to the severe sign problem. This could make trouble with the analysis of interaction vertex Γ; it is possible that the strengths of the spin and charge fluctuations which contribute to Γ changes as temperature is lowered, since the spin susceptibility $\chi_{\mathrm{s}}(\boldsymbol{Q})$ grows rapidly while the charge susceptibility $\chi_{\mathrm{c}}(\pi,\pi)$ shows more moderate behavior in the temperature range we calculated (not shown). Thus, the effect of V on SC symmetry at lower temperatures still remains open. We hope that more studies would be carried out both from theoretical and experimental point of view.

Acknowledgment

We are grateful to T. Kato and Y. Uwatoko for helpful discussions. The present work was financially supported by Grants-in-Aid for Scientific Research on Priority Areas of Molecular Conductors (No. 15073210) from the Ministry of Education, Culture, Sports, Science and Technology, Japan (MEXT), and Next Generation Supercomputing Project, Nanoscience Program, MEXT. Y.F. is supported by JSPS Research Fellowships for Young Scientists. The computation in this work has been done using the facilities of the Supercomputer Center, Institute for Solid State Physics, University of Tokyo.

1) D. Jérome, A. Mazuad, M. Ribault, and K. Bechgaard: J. Phys. Lett. **41** (1980) L95.
2) D. Jérome: Science **252** (1991) 1509.
3) V. J. Emery: Synth. Met. **13** (1986) 21.
4) H. Shimahara: J. Phys. Soc. Jpn. **58** (1989) 1481.
5) H. Kino and H. Kontani: J. Phys. Soc. Jpn. **68** (1999) 1481.
6) H. Kino and H. Kontani: J. Low Temp. Phys. **117** (1999) 317.
7) R. Duprat and C. Bourbonnais: Eur. Phys. J. B **21** (2001) 219.
8) M. Itoi, C, Araki, M. Hedo, Y. Uwatoko and T. Nakamura: J. Phys. Soc. Jpn. **77** (2008) 023701.
9) Y. Suzumura and H. Fukuyama: J. Low Temp. Phys. **31** (1978), 273.
10) Y. Fuseya, M. Tsuchiizu, Y. Suzumura and C. Bourbonnais: J. Phys. Soc. Jpn. **76** (2007) 014709.
11) Y. Fuseya and Y. Suzumura: J. Phys. Soc. Jpn. **74** (2005) 1263.
12) Y. Fuseya and M. Ogata: J. Phys. Soc. Jpn. **76** (2007) 093701.
13) N. E. Bickers and S. R. White: Phys. Rev. B **43** (1991) 8044.
14) J. E. Hirsch: Phys. Rev. B **31** (1985) 4403.
15) S. R. White, D. J. Scalapino, R. L. Sugar, E. Y. Loh, J. E. Gubernatis and R. T. Scalettar: Phys. Rev. B **40** (1989) 506.
16) H. Seo, C. Hotta and H. Fukuyama: Chem. Rev. **104** (2004) 5005.
17) H. Seo, J. Merino, H. Yoshioka and M. Ogata: J. Phys. Soc. Jpn. **75** (2006) 051009.
18) A. Kobayashi, S. Katayama, K. Noguchi and Y. Suzumura: J. Phys. Soc. Jpn. **73** (2004) 3135.
19) A. Kobayashi, Y. Tanaka, M. Ogata and Y. Suzumura: J. Phys. Soc. Jpn. **73** (2004) 1115.
20) A. Kobayashi, S. Katayama and Y. Suzumura: J. Phys. Soc. Jpn. **74** (2005) 2897.
21) K. Yoshimi, M. Nakamura and H. Mori: J. Phys. Soc. Jpn. **76** (2007) 024706.
22) V. Vescoli, L. Degiorgi, W. Henderson, G. Grüner, K. P. Starkey and L. K. Montgomery: Science **281** (1998) 1181.
23) H. Yoshioka, M. Tsuchiizu and Y. Suzumura: J. Phys. Soc. Jpn. **70** (2001) 762.
24) M. Tsuchiizu, H. Yoshioka and Y. Suzumura: J. Phys. Soc. Jpn. **70** (2001) 1460.
25) Y. Zhang and J. Callaway: Phys. Rev. B **39** (1989) 9397.
26) T. Koretsune and M. Ogata: J. Phys. Soc. Jpn. **74** (2005) 1390.
27) T. Koretsune and M. Ogata: Phys. Rev. B **72** (2005) 134513.
28) S. R. White, D. J. Scalapino, R. L. Sugar, N. E. Bickers and R. T. Scalettar: Phys. Rev. B **39** (1989) 839.
29) M. Jarrell and J. E. Gubernatis: Phys. Rep. **269** (1996) 133.
30) L. Ducasse, M. A. Abderrabba, J. Hoarau, M. Pesquer, B. Gallois and J. Gaultier: J. Phys. C **19** (1986) 3805.
31) It should be noted that the charge fluctuation is also affected by the shape of the Fermi surface. For example, $\chi_{\mathrm{c}}(\boldsymbol{q})$ is given as $\chi_{\mathrm{c}}(\boldsymbol{q}) = \chi_0(\boldsymbol{q})/(1+V(\boldsymbol{q})\chi_0(\boldsymbol{q}))$ within RPA, which clearly shows that $\chi_{\mathrm{c}}(\boldsymbol{q})$ is affected by the nesting property through $\chi_0(\boldsymbol{q})$. In fact, out result of $\chi_{\mathrm{c}}(\boldsymbol{q})$ for $V=0$ slightly reflects

the shape of the Fermi surface. However, the effect of $V(\boldsymbol{q})$ is stronger than that of $\chi_0(\boldsymbol{q})$. This leads to the emergence of $\boldsymbol{q} = (\pi, \pi)$ charge disproportionation under the presence of V which reflects the lattice structure rather than the nesting condition.